doi:10.1093/plphys/kiab362 PLANT PHYSIOLOGY 2021: 187: 1713–1727

Plant Physiology®

Research Article

Jasmonates modulate sphingolipid metabolism and accelerate cell death in the ceramide kinase mutant *acd5*

Li-Qun Huang,[1] Ding-Kang Chen,[1] Ping-Ping Li ,[1] He-Nan Bao ,[1] Hao-Zhuo Liu,[1] Jian Yin,[1] Hong-Yun Zeng,[1] Yu-Bing Yang,[1] Yong-Kang Li,[1] Shi Xiao [1] and Nan Yao [1,*,†]

1 State Key Laboratory of Biocontrol, Guangdong Provincial Key Laboratory of Plant Resources, School of Life Sciences, Sun Yat-sen University, Guangzhou 510275, P.R. China

*Author for communication: yaonan@mail.sysu.edu.cn
†Senior author.

L.Q.H. and N.Y. contributed to the conception of this work and wrote the manuscript; L.Q.H. conducted most of the experiments; S.X. and N.Y. contributed reagents/materials/analysis tools. L.Q.H., D.K.C., H.Z.L., and J.Y. conducted the sphingolipid detection and analysis; L.Q.H., D.K.C., and Y.K.L. measured hormones. L.Q.H. and P.P.L. contributed to the insect feeding assay; L.Q.H., Y.B.Y., and H.Y.Z. contributed to the mutant construction; L.Q.H. and H.N.B. contributed to the investigation of fungal resistance.
The author responsible for distribution of materials integral to the findings presented in this article in accordance with the policy described in the Instructions for Authors (https://academic.oup.com/plphys/pages/General-Instructions) is: Nan Yao (yaonan@mail.sysu.edu.cn).

Abstract

Sphingolipids are structural components of the lipid bilayer that acts as signaling molecules in many cellular processes, including cell death. Ceramides, key intermediates in sphingolipid metabolism, are phosphorylated by the ceramide kinase ACCELERATED CELL DEATH5 (ACD5). The loss of ACD5 function leads to ceramide accumulation and spontaneous cell death. Here, we report that the jasmonate (JA) pathway is activated in the Arabidopsis (*Arabidopsis thaliana*) *acd5* mutant and that methyl JA treatment accelerates ceramide accumulation and cell death in *acd5*. Moreover, the double mutants of *acd5* with *jasmonate resistant1-1 and coronatine insensitive1-2* exhibited delayed cell death, suggesting that the JA pathway is involved in *acd5*-mediated cell death. Quantitative sphingolipid profiling of plants treated with methyl JA indicated that JAs influence sphingolipid metabolism by increasing the levels of ceramides and hydroxyceramides, but this pathway is dramatically attenuated by mutations affecting JA pathway proteins. Furthermore, we showed that JAs regulate the expression of genes encoding enzymes in ceramide metabolism. Together, our findings show that JAs accelerate cell death in *acd5* mutants, possibly by modulating sphingolipid metabolism and increasing ceramide levels.

Introduction

Plant sphingolipids make up an estimated 40% of plasma membrane lipids; sphingolipids also regulate cellular processes and responses to environmental stresses (Berkey et al., 2012; Luttgeharm et al., 2016; Ali et al., 2018). The key intermediates in sphingolipid biosynthesis and catabolism are ceramides, which consist of a long-chain amino alcohol, referred to as a sphingoid long-chain base (LCB), and a fatty acid (FA) of variable length (Luttgeharm et al., 2016).

Received June 24, 2021. Accepted July 09, 2021. Advance access publication August 7, 2021

Ceramides mediate plant programmed cell death (PCD; Liang et al., 2003; Townley et al., 2005; Wang et al., 2008; Ternes et al., 2011; Bi et al., 2014; Simanshu et al., 2014); for example, treatment with exogenous C2 ceramide (ceramide with a C2 FA) leads to calcium-dependent PCD in Arabidopsis (*Arabidopsis thaliana*; Townley et al., 2005). The loss of function of the ceramide-1-phosphate transporter in the *accelerated cell death11* (*acd11*) mutant leads to ceramide accumulation and salicylic acid (SA)-dependent PCD (Simanshu et al., 2014). Moreover, mutation of the ceramide synthase gene *LONGEVITY ASSURANCE GENE ONE HOMOLOG1* (*LOH1*) results in increased levels of trihydroxy sphingoid bases, C16 ceramides, and C16 glucosylceramide species, and leads to spontaneous cell death (Ternes et al., 2011).

ACCELERATED CELL DEATH5 (*ACD5*) encodes a ceramide kinase that catalyzes the conversion of ceramide to ceramide-1-phosphate; the *acd5* mutation causes SA-pathway-dependent ceramide accumulation and spontaneous cell death late in development (Greenberg et al., 2000; Liang et al., 2003, Bi et al., 2014). Treatment with SA or its analog benzothiadiazole (BTH) accelerates cell death in *acd5* mutants and the cell death phenotype is attenuated in the *acd5 NahG and acd5 nonexpresser of pathogenesis-related genes1-1* (*npr1-1*) double mutants (Greenberg et al., 2000; Yang et al., 2019). Furthermore, ethylene signaling is partially required for *acd5*-conferred cell death (Greenberg et al., 2000). In contrast, abscisic acid (ABA) suppresses the cell death phenotype of the *acd5* mutant after BTH induction (Yang et al., 2019). Thus, phytohormones play important and varying roles in sphingolipid-induced cell death.

Jasmonates (JAs) are also involved in cell death caused by sphingolipid imbalances. The fungal toxin fumonisin B1 (FB1) inhibits sphingolipid biosynthesis, leading to cell death, in a process requiring a functional JA pathway (Asai et al., 2000). Moreover, disruption of neutral ceramidases 1 and 2 also results in JA-pathway-associated cell death (Zienkiewicz et al., 2019). However, the mechanism by which JAs participate in sphingolipid-induced cell death has remained unknown, along with the role of the JA pathway in the lesion-mimic mutant *acd5*.

JAs, a family of lipid-derived phytohormones, are ubiquitous in land plants and play an important role in stress responses and development (Howe et al., 2018). Among them, (+)-7-*iso*-jasmonoyl-L-isoleucine (JA-Ile) is the bioactive compound, which is synthesized by jasmonoyl amino acid conjugate synthase (JASMONATE RESISTANT1, JAR1; Fonseca et al., 2009). The core JA signaling pathway consists of interconnected functional modules that govern the transcriptional state of hormone-responsive genes. The basic helix-loop-helix transcription factors MYC2, MYC3, and MYC4 are repressed by JASMONATE-ZIM-DOMAIN (JAZ) proteins when the endogenous levels of JA-Ile are low (Howe et al., 2018). When JA-Ile levels rise, the JA-Ile receptor CORONATINE INSENSITIVE1 (COI1) binds to JAZs and causes their ubiquitination and degradation, releasing the transcription factors to activate the expression of downstream genes (Xie et al., 1998; Thines et al., 2007; Yan et al., 2009). MEDIATOR25 (MED25) is a subunit of the mediator transcriptional co-activator complex, which controls MYC2-dependent transcription, and the MYC2–MED25 transcriptional complex plays a critical role in the activation and termination of JA signaling (Chen et al., 2012; An et al., 2017; Du et al., 2017; Liu et al., 2019).

JAs function in plant resistance to necrotrophic pathogens and insects (Howe et al., 2018). Previous reports suggested that disturbance of sphingolipid metabolism affects plant tolerance to the insect herbivore brown planthopper (*Nilaparvata lugens*) and aphids (*Myzus persicae*), as well as the necrotrophic fungal pathogen *Botrytis cinerea* (Magnin-Robert et al., 2015; Begum et al., 2016). Sphingolipid profiles are altered upon *B. cinerea* infection (Bi et al., 2014; Magnin-Robert et al., 2015). Nevertheless, the direct connection between the JA pathway and sphingolipid metabolism has remained poorly understood.

In this work, we investigated the effects of JA on the *acd5* mutant. We treated *acd5* plants with exogenous methyl jasmonate (MeJA) and found it enhanced the cell death phenotype. By analyzing sphingolipid profiling, we showed that MeJA treatment triggered an increase in ceramide and hydroxyceramide levels in a JA-pathway-dependent manner. We suggest that JAs accelerate cell death in the ceramide kinase mutant *acd5* by modulating sphingolipid metabolism.

Results

The JA pathway is activated in *acd5* mutants

To explore the association between the JA pathway and ACD5 function, we investigated the transcript levels of JA-related genes in *acd5* at different developmental stages. In 16-d-old plants, the expression of the JA biosynthesis genes *ALLENE OXIDE SYNTHASE* (*AOS*), *MYC2*, and *12-OXOPHYTODIENOATE REDUCTASE3* (*OPR3*) and the JA signaling pathway gene *JAZ1* was not upregulated in *acd5* compared with the wild-type. However, the JA-responsive gene *PDF1.2* showed higher transcript levels in *acd5* than in the wild-type (Figure 1A). In 32-d-old *acd5* plants, all five of these JA-related genes were significantly upregulated (Figure 1A). Furthermore, in 16-d-old plants, the contents of jasmonic acid, JA-Ile, the JA precursor 12-oxophytodienoic acid (OPDA), SA, and its storage form salicylic acid O-β-glucoside (SAG) were similar between the wild-type and *acd5* (Figure 1B; Supplemental Figure S1). At 32 d, however, JA levels were dramatically higher in the *acd5* mutant than in the wild-type (Figure 1B), and as described previously, the *acd5* mutants accumulated SA in late developmental stages (Greenberg et al., 2000; Supplemental Figure S1).

Ceramide accumulation is a key feature of the *acd5* mutant (Liang et al., 2003; Bi et al., 2014). To assess whether ceramide accumulation could increase the transcript levels of JA pathway genes, we treated 7-d-old wild-type seedlings with exogenous C2-ceramide and C16-ceramide. These treatments resulted in increased expression of *AOS*, *OPR3*, *MYC2*,

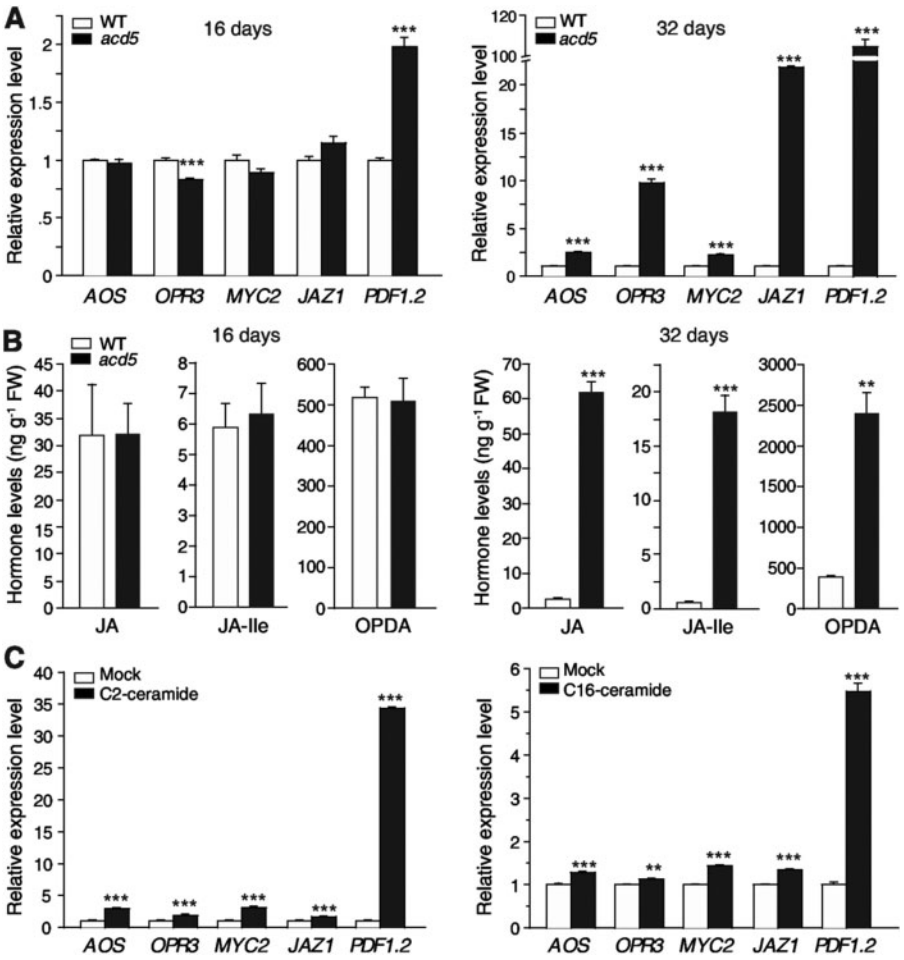

Figure 1 JA-related gene expression and plant hormone contents in *acd5* mutant plants. **A**, Expression of jasmonate-pathway-related genes in *acd5* plants, as indicated by RT-qPCR analyses of *AOS*, *OPR3*, *MYC2*, *JAZ1*, and *PDF1.2* transcript levels in the wild-type and *acd5* plants sampled at 16 and 32 d of age. *ACT2* transcript levels were used as the internal control. Gene expression values are relative to the average for wild-type plants (set as 1). **B**, Levels of the hormones JA, JA-Ile, and OPDA in 16- and 32-d-old wild-type and *acd5* plants. Note no cell death phenotype in 16-d-old *acd5* plants. **C**, Expression of JA-pathway-related genes after ceramide treatments. Seven-day-old wild-type seedlings were treated with 50-μM C2- or C16-ceramide. The samples were collected after 6 h and used for RNA isolation. The JA biosynthesis genes *AOS*, *OPR3*, and JA downstream genes *MYC2*, *JAZ1*, and *PDF1.2* were assayed by RT-qPCR. *ACT2* transcript levels were used as the internal control. Gene expression values are relative to the average for mock (1% ethanol)-treated wild-type (set as 1). These experiments were repeated at least three times using independent samples. Data represent means ± SE from triplicate biological replicates. Significant differences were determined by Student's *t* tests (*$P < 0.05$, **$P < 0.01$; ***$P < 0.001$).

JAZ1, and *PDF1.2* (Figure 1C). Taken together, these data suggested that ceramide accumulation induces the expression of JA pathway genes.

acd5 mutants uncouple JA-associated gene expression and stress responses

Because the *acd5* mutant had higher expression of JA-related genes and JA contents than the wild-type, we hypothesized that it would have correspondingly greater resistance to insect herbivory and necrotrophic pathogens. However, as shown in Figure 2, we found no difference in phenotype between the wild-type and *acd5* mutant after challenge by larvae of the beet armyworm *Spodoptera exigua* (Figure 2A). No significant difference was detected in weight between *S. exigua* larvae that fed on the wild-type and *acd5* plants (Figure 2B), despite herbivory-induced increases in the transcript levels of the defense genes *JAZ10* and *TAT1* and in the endogenous levels of jasmonic acid in *acd5* as compared to the wild-type (Figure 2, C and D). We also checked JA-associated gene expression levels after *B. cinerea* inoculation. Consistent with a previous report (Bi et al., 2014), the *acd5* plants were susceptible to *B. cinerea* (Supplemental Figure S2A). However, higher expression of *ALLENE OXIDE CYCLASE1* (*AOC1*) and *PDF1.2* compared with the wild-type was found at 12 h after inoculation (Supplemental Figure S2B).

Furthermore, upon treatment with 100-μM MeJA, the *acd5* mutant plants did not show more severe root-growth inhibition or anthocyanin accumulation than the wild-type (Figure 2, E and F). Thus, notwithstanding the JA pathway activation seen in the *acd5* mutant, the resistance to JA-related biotic stress was not enhanced, and the MeJA-

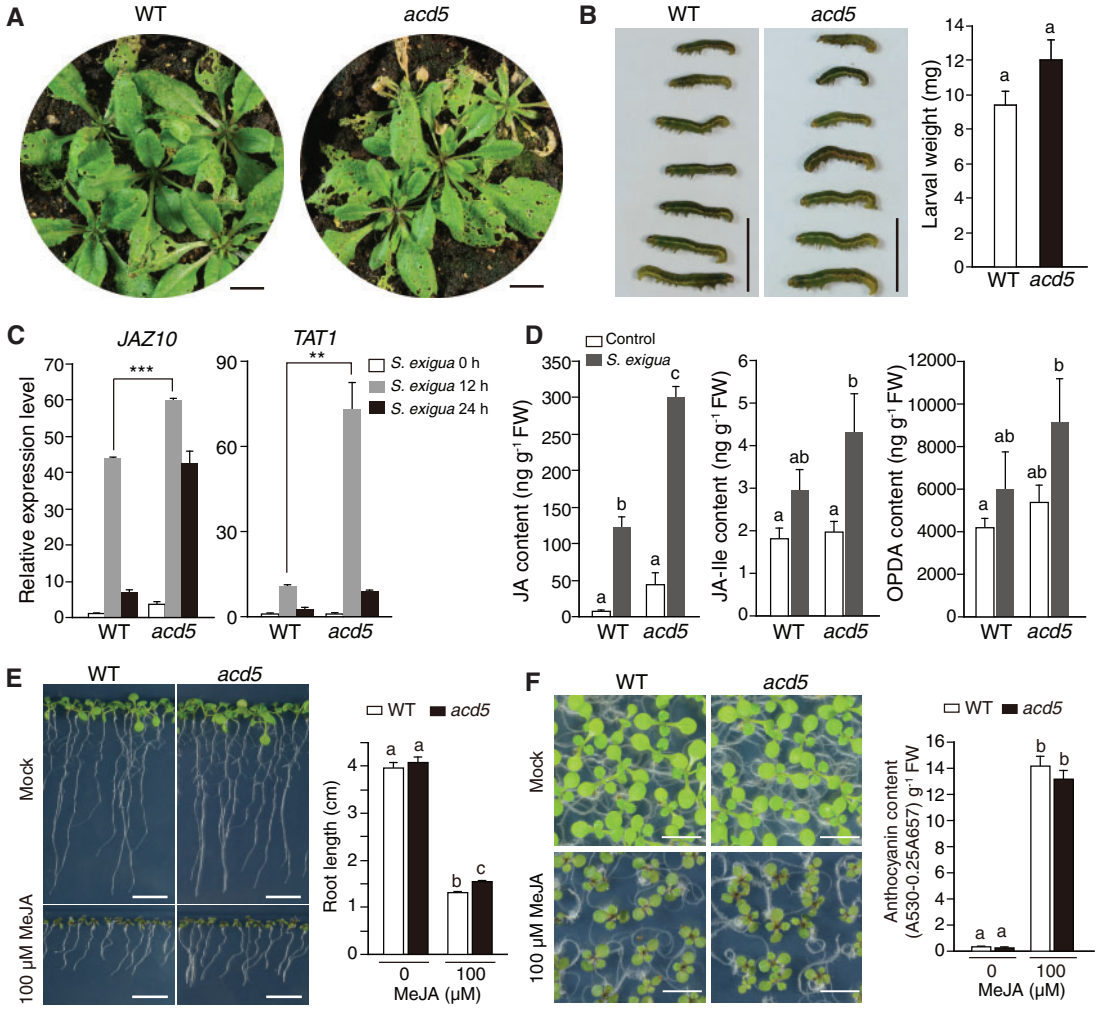

Figure 2 Function of ACD5 in *S. exigua* resistance and JA-associated developmental responses. A and B, Insect bioassay on the wild-type and *acd5* plants. A, Second-instar *S. exigua* larva were released on 4-week-old plants. Photographs of plants were taken 8 d after insect release. **B**, Larval weights of *S. exigua* were measured 8 d after release on the wild-type and *acd5* plants. Data represent means ± SE ($n \geq 20$ larvae per genotype); different letters in (B) represent significant differences from the wild-type as determined using Student's *t* tests ($P < 0.05$). **C**, Expression of *JAZ10 and TAT1* in the wild-type and *acd5* plants after *S. exigua* herbivory. Data represent means ± SE using independent samples ($n = 3$). Significant differences were determined by Student's *t* tests (**$P < 0.01$; ***$P < 0.001$). **D**, Analysis of JA, JA-Ile, and OPDA contents in plants challenged by *S. exigua* second-instar larvae for 24 h and then collected for analysis. Data represent means ± SE using independent samples ($n = 3$); different letters indicate significant differences determined by ANOVA with post hoc test ($P < 0.05$). **E**, JA-inhibited root growth phenotypes of the wild-type and *acd5* plants. Ten-day-old seedlings grown on 1/2 MS medium with or without 100-μM MeJA were photographed. Data represent means ± SE ($n \geq 40$ seedlings per genotype). Different letters indicate significant differences determined by ANOVA with post hoc test ($P < 0.05$). **F**, The accumulation of anthocyanin in response to JA in the wild-type and *acd5* plants grown on 1/2 MS medium with or without 100 μM MeJA. Representative photos show seedlings after 10 d, and their anthocyanin contents are at right. Data represent means ± SE ($n = 10$). Datasets marked with different letters indicate significant differences assessed by ANOVA with post hoc test ($P < 0.05$). Experiments were repeated at least three times (**A**–**E**) or twice (**F**). Scale bars, 1 cm (**A**, **B**, and **E**), 0.5 cm (**F**).

induced root-growth inhibition and anthocyanin accumulation were not increased in the *acd5* plants.

MeJA accelerates ceramide accumulation and cell death in *acd5* mutants

The *acd5* mutant eventually shows spontaneous cell death (Greenberg et al., 2000), accompanied by increases in gene transcripts and hormones associated with the JA pathway. To investigate whether the JA pathway functions in this spontaneous cell death process, we sprayed the wild-type and *acd5* plants with exogenous MeJA. Treatment with 50-μM MeJA had no significant effect on the cell death phenotype of the *acd5* plants (Supplemental Figure S3A), as determined by phenotypic analyses and electrolyte leakage assays (Supplemental Figure S3, B and C). However, treatment with 100-μM MeJA accelerated spontaneous cell death and increased electrolyte leakage levels in the *acd5* mutant, but

not the wild-type, at the indicated time points after treatment, compared with the mock-treated plants given 0.1% ethanol (Figure 3, A–C). Treatment with 200-μM MeJA further worsened cell death in the *acd5* plants, while still not causing cell death in the wild-type (Supplemental Figure S3, A and C), indicating that the JA-induced acceleration of cell death in the *acd5* mutant was dose dependent. Moreover, MeJA treatment induced the transcript levels of defense-, senescence-, and reactive oxygen species-related genes in *acd5* plants, and the JA and SA contents increased in MeJA-treated *acd5* mutants 10 d after treatment (Supplemental Figures S4 and S5). These data further demonstrated that MeJA induces cell death in *acd5* and this process is closely related to the plant hormones JA and SA.

Ceramide accumulation is a key factor in the timing of the *acd5* cell death phenotype (Bi et al., 2014). We measured the sphingolipid profiles of the wild-type and *acd5*, with or without 100-μM MeJA treatment. In line with our expectations, MeJA treatment increased the total amount of ceramides and hydroxyceramides in the *acd5* plants (Figure 3, D and F), and it induced the accumulation of individual ceramide and hydroxyceramide species in *acd5* (Figure 3, E and G). Taking these observations together, our results showed that exogenous MeJA treatment accelerated both cell death and sphingolipid accumulation in the *acd5* mutant.

As described in a previous study, exogenous C2-ceramide induced cell death of wild-type protoplasts (Liang et al., 2003). To investigate the effect of MeJA on ceramide-induced cell death, we treated protoplasts from wild-type plants with ceramides and MeJA. Treatment with C2-ceramide or MeJA was sufficient to induce cell death in Arabidopsis (Supplemental Figure S6). However, treatment with C2-ceramide and MeJA together induced cell death of wild-type protoplasts more strongly than C2-ceramide or MeJA alone, which indicated that MeJA accelerates ceramide-induced cell death at the cellular level (Supplemental Figure S6).

The JA pathway contributes to SA-dependent cell death in *acd5*

To confirm the roles of the JA pathways in MeJA-induced cell death in *acd5*, we examined the relative expression levels of JA-related genes after treatment with 100-μM MeJA. In line with the data in Figure 1, JA pathway genes were not induced in untreated 16-d-old *acd5* plants (Supplemental Figure S7A). The JA biosynthesis genes *AOS and OPR3* and the JA signaling pathway gene *JAZ1* were upregulated in both the wild-type and *acd5* plants 2 d after MeJA treatment (Supplemental Figure S7B). In contrast, the transcript levels of the SA-related genes *SALICYLIC ACID INDUCTION DEFICIENT2* (*SID2*), *ENHANCED DISEASE SUSCEPTIBILITY1* (*EDS1*), and *PHYTOALEXIN DEFICIENT4* (*PAD4*) showed no difference between the mock- and MeJA-treated *acd5* plants (Supplemental Figure S7B), suggesting that the JA pathway plays an important role in accelerating the development of the *acd5* phenotype in early stages, 2 d after MeJA treatment. At 8 d after MeJA treatment, most of the JA- and SA-related genes were significantly upregulated in MeJA-treated *acd5* plants as compared to mock-treated *acd5* mutants (Supplemental Figure S7C).

To further investigate the contribution of the JA pathway to the cell death phenotype of the *acd5* mutant, we introduced the JA pathway mutants *jar1-1*, *coi1-2*, and *myc2-2* (Staswick et al., 2002; Xiao et al., 2004; Boter et al., 2004; Yuan et al., 2017) into the *acd5* background. The *acd5 myc2-2* double mutant did not show rescue of cell death (Figure 4A), with almost 55% of plants showing the cell death phenotype at 4 weeks after germination, similar to the percentage for *acd5* plants (Supplemental Figure S8A). Moreover, the cell death lesions in the *acd5 myc2-2* mutants were severe and widespread, as detected by trypan blue staining (Figure 4B). In contrast, introducing *jar1-1* or *coi1-2* into the *acd5* mutant delayed the appearance of the cell death phenotype, so that fewer plants showed spontaneous cell death at 4 weeks (Figure 4A; Supplemental Figure S8A). Although the loss of function of JAR1 or COI1 delayed the development of the *acd5* phenotype, the cell death lesions appeared and spread in both double mutants by 5 weeks (Figure 4, A and B). The double mutants also exhibited the cell death phenotype in stems, which is typical of *acd5* mutants at 6 weeks after planting (Supplemental Figure S8B).

We also measured the sphingolipid contents in 4- and 5-week-old plants. The total amount of ceramides was higher in 4-week-old *acd5 and acd5 myc2-2* plants, but not *acd5 coi1-2* or *acd5 jar1-1* plants (Figure 4C). In addition, the levels of different individual ceramides were significantly higher in *acd5 and acd5 myc2-2* compared with the wild-type, which was consistent with the total ceramide levels (Figure 4D). All of the 5-week-old plants in the *acd5* background showed increases in total ceramides and individual ceramide species, but the sphingolipid content was generally lower in *acd5 jar1-1* than in *acd5* plants (Figure 4, C and E). Taken together, these results indicate that the cell death seen in *acd5* is partly dependent on the JA pathway.

To investigate the relationship between the JA and sphingolipid pathways, and to determine the role of the JA pathway in accelerating the cell death phenotype of *acd5*, we treated wild-type plants and JA pathway mutants with 100-μM MeJA. At 2 d after MeJA treatment, the levels of total LCBs, glucosylceramides (GlcCers), and glycosylinositol phosphorylceramides (GIPCs) were not significantly changed in wild-type plants, although, interestingly, the total ceramide and hydroxyceramide contents increased in wild-type plants (Figure 5A). Consistent with the total amount of sphingolipids, the levels of individual ceramide and hydroxyceramide species increased only in wild-type plants (Figure 5, B and C; Supplemental Figure S9). Nevertheless, in the *coi1-2 and jar1-1* mutants, the levels of ceramides and hydroxyceramides were not increased by exogenous MeJA treatment (Figure 5; Supplemental Figure S9, A and B). However, the

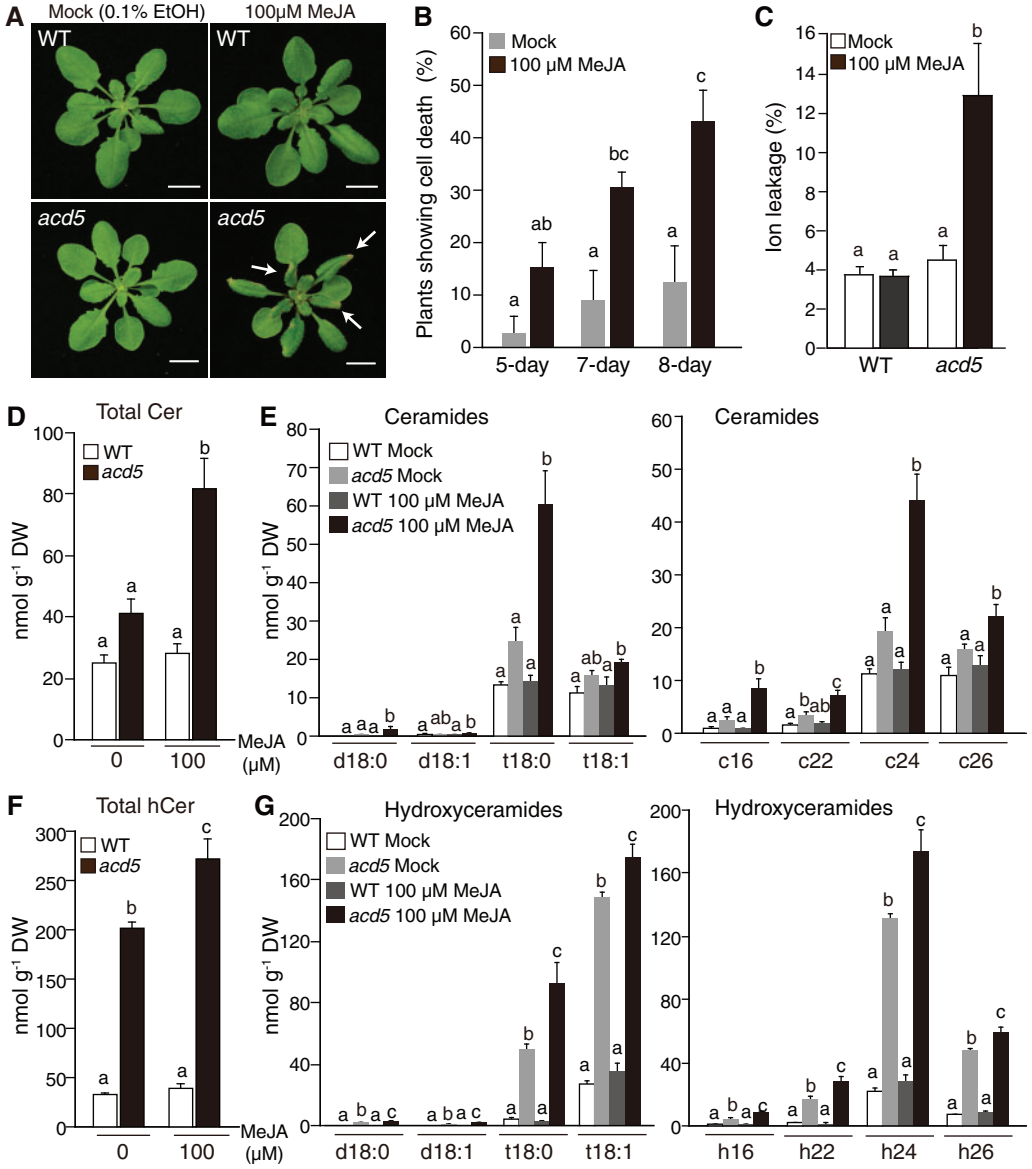

Figure 3 Effect of MeJA treatment on the cell death phenotype of *acd5*. Sixteen-day-old wild-type and *acd5* plants were sprayed with solvent control (0.1% ethanol) or 100-μM MeJA. Scale bars in (A) = 1 cm. Different letters indicate significant differences determined by ANOVA with post hoc test ($P < 0.05$). A, MeJA treatment accelerates the cell death phenotype of *acd5* mutants. Photographs were taken 10 d after spraying. The arrows indicate leaves showing cell death lesions typical of *acd5* plants. B, The proportion (as a percentage of the total) of *acd5* plants showing the cell death phenotype after MeJA treatment. Data represent means ± SE from two biological replicates. At least 150 plants were observed for each treatment. C, The electrolyte leakage in the wild-type and *acd5* plants 10 d after MeJA treatment. Data represent means ± SE using independent samples ($n = 6$). These experiments were repeated at least three times. D–G, Sphingolipid profiles in the wild-type and *acd5* plants 10 d after spraying 100-μM MeJA. Total contents of ceramides (Cer) (D) and hydroxyceramides (hCer) (F) were measured. Ceramide species (E) and hydroxyceramide species (G) with LCB moieties (left) and FA moieties (right) were also analyzed. Data represent means ± SE using independent samples ($n = 3$). These experiments were repeated at least three times.

loss of function of *MYC2* in the wild-type had no effect on the JA-induced accumulation of ceramides and hydroxyceramides (Figure 5D; Supplemental Figure S9C). We thus concluded that JAs modulate the contents of ceramides and hydroxyceramides through mechanisms that are dependent on the normal functions of JAR1 and COI1.

Treatment with 100-μM MeJA did not cause cell death in the wild-type or in JA and SA pathway mutants (Supplemental Figure S10). Next, we sprayed 100-μM MeJA on *acd5*, *acd5 coi1-2*, *acd5 jar1-1*, *acd5 npr1-1*, and *acd5 NahG* plants and recorded the proportion of plants showing the cell death phenotype. The results showed that the loss of function of *COI1* or *JAR1* in the *acd5* mutant significantly suppressed MeJA-induced acceleration of the cell death in *acd5* (Figure 6, A–C). The spread of cell death lesions in the *acd5 coi1-2 and acd5 jar1-1* double mutants showed similar patterns with or without MeJA treatment, as observed by trypan blue staining (Figure 6B). Furthermore, with or

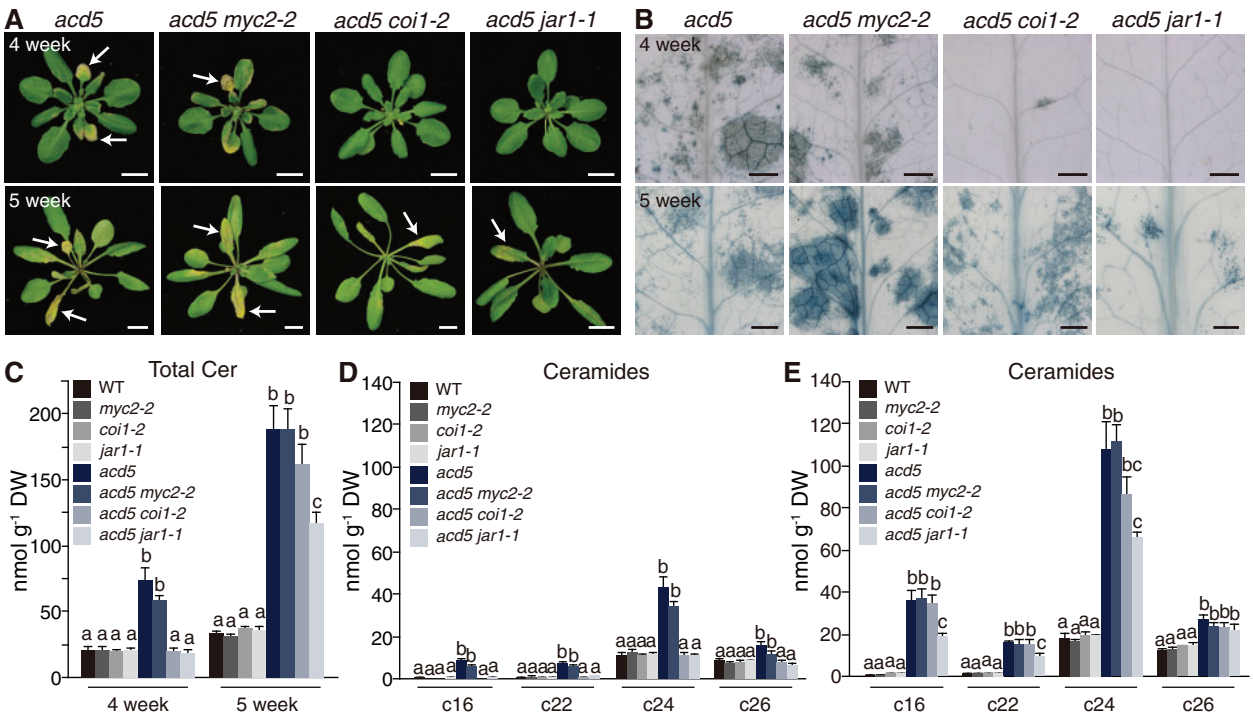

Figure 4 Effect of JA pathway mutations on the cell death phenotype and ceramide accumulation of the *acd5* mutant. A, Phenotypes of 4- and 5-week-old soil-grown Arabidopsis plants. Arrows indicate cell death lesions. Scale bars, 1 cm. B, Representative microscopic images of trypan blue staining of 4- and 5-week-old plants as shown in (A). Bars, 1 mm. C–E, The amounts of ceramides in the wild-type and indicated mutant plants. Total contents of ceramides in 4- and 5-week-old plants were measured (C). Ceramide species with FA moieties in 4- (D) and 5-week-old plants (F) were analyzed. Data represent means ± SE from independent samples ($n = 3$). Different letters indicate significant differences determined by ANOVA with post hoc test ($P < 0.01$). These experiments were repeated at least three times.

without MeJA treatment, the *acd5 npr1-1 and acd5 NahG* plants showed no cell death phenotype (Figure 6, D–F), again confirmed that the spontaneous cell death phenotype of *acd5* is largely dependent on the SA pathway (Greenberg et al., 2000). We conclude that JA accelerated the cell death in *acd5* mutants by a mechanism that was dependent on the presence of intact JA and SA signaling pathways.

JAs are involved in regulating ceramide metabolism

To further explore the mechanism by which JA accelerates the cell death in *acd5* mutants through regulating ceramide metabolism, we treated wild-type plants with 100-μM MeJA and detected the transcript levels of genes involved in ceramide synthesis and degradation. Arabidopsis has three ceramide synthase gene homologs, *LOH1*, *LOH2*, and *LOH3* (Ternes et al., 2011). Our data showed that 6 h after MeJA treatment, the expression of *LOH1 and LOH2* was significantly induced (Figure 7A). Moreover, the expression of *ARABIDOPSIS TURGOR REGULATION DEFECT1* (*TOD1*), which encodes an alkaline ceramidase that degrades ceramides into LCBs and FAs, was significantly decreased (Figure 7A; Chen et al., 2015), indicating that the transcript level of *TOD1* was inhibited by MeJA treatment. We also found that the expression of *ACD5* itself was upregulated under MeJA treatment (Figure 7A). In *acd5* mutants, the expression of genes involved in ceramide metabolism was also regulated by MeJA treatment (Supplemental Figure S11).

Furthermore, MYC2 is the master transcription factor in JA signaling, and its function depends on its interaction with MED25 (Chen et al., 2012). To test the effect of MYC2 on the expression of *ACD5*, we cloned the ~1,700-bp *ACD5* promoter sequence into the pGreenII 0800-LUC vector to generate the $ACD5_{pro}$-*LUC* reporter construct (Supplemental Figure S12A). The coexpression of MYC2 with $ACD5_{pro}$-*LUC* in Arabidopsis protoplasts led to significantly increased luciferase (LUC) activity (Supplemental Figure S12B). This result demonstrated that MYC2 is involved in regulating the expression of the ceramide kinase gene *ACD5*. Moreover, we found that the transcript levels of *MYC2 and MED25* increased in *acd5* plants 10 d after MeJA treatment, which indicated that the MYC2–MED25 transcriptional complex plays an important role in MeJA-induced ceramide accumulation and cell death in *acd5* mutants (Supplemental Figure S4). Taking these results together, we proposed our current working model as shown in Figure 7B. The JA pathway may be involved in the transcriptional regulation of genes related to ceramide metabolism.

Discussion

Previous reports have suggested that plant hormones such as SA, ABA, and ethylene mediate spontaneous cell death in the *acd5* mutant (Greenberg et al., 2000; Bi et al., 2014; Yang et al., 2019), but the role of the JA in cell death processes was not clear. In this study, we found that *acd5*

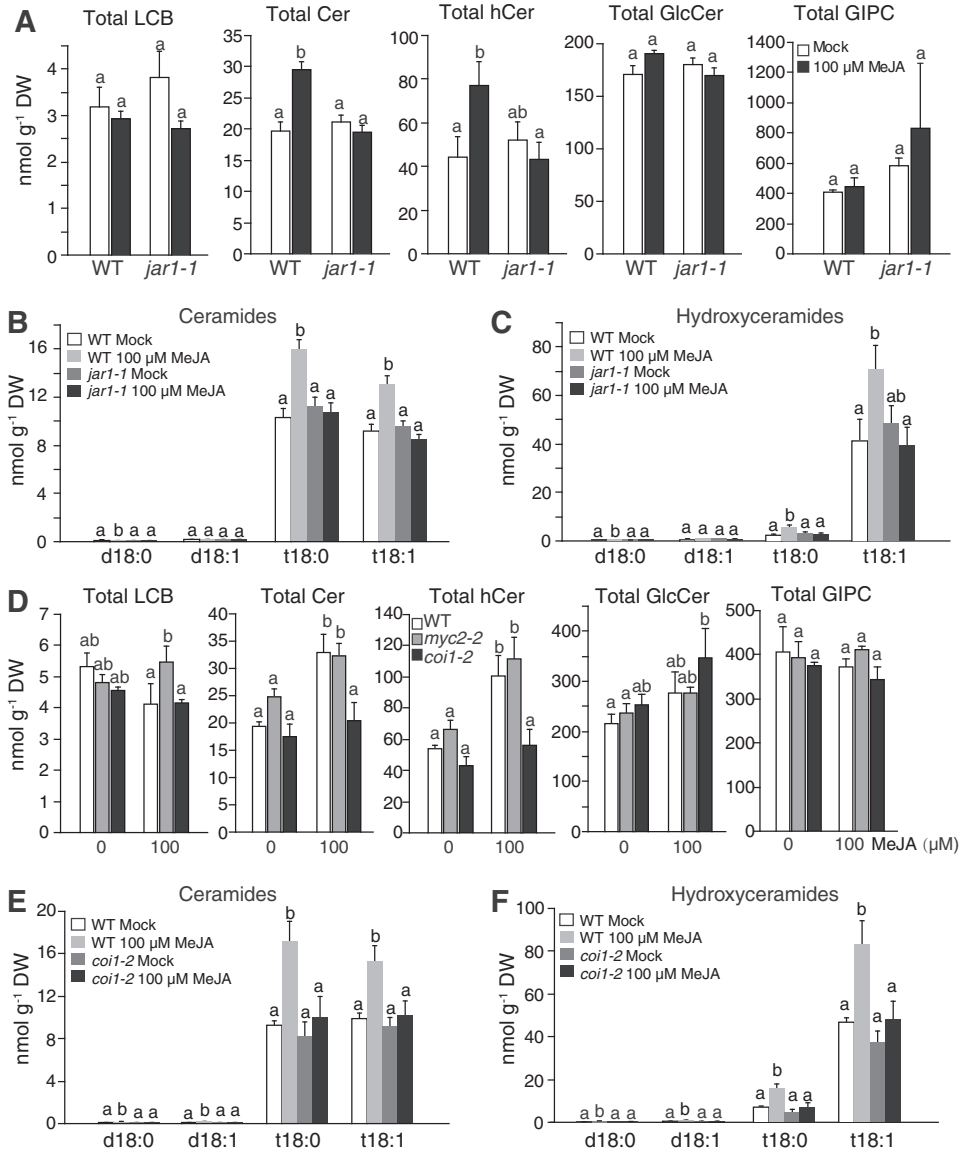

Figure 5 Sphingolipid contents of JA pathway mutants after MeJA treatment. Twenty-one-day-old wild-type, *jar1-1*, *myc2-2*, and *coi1-2* plants were sprayed with mock-treatment solution (0.1% ethanol) or 100-μM MeJA. Samples were collected 2 d after treatment. Data represent means ± SE using independent samples ($n = 3$). These experiments were repeated at least three times. Different letters indicate significant differences determined by ANOVA with post hoc test ($P < 0.05$). A, Total contents of LCB, ceramides (Cer), hydroxyceramides (hCer), glucosylceramides (GlcCer), and GIPCs in wild-type and *jar1-1* plants with or without MeJA. B, Ceramide species with LCB moieties in wild-type and *jar1-1* plants. C, Hydroxyceramide species with LCB moieties in wild-type and *jar1-1* plants. D, Total contents of LCB, Cer, hCer, GlcCer, and GIPC in wild-type, *myc2-2*, and *coi1-2* plants after MeJA treatment. E, Ceramide species with LCB moieties in wild-type and *coi1-2* plants after MeJA treatment. F, Hydroxyceramide species with LCB moieties in wild-type and *coi1-1* plants.

plants had increased transcript levels of JA pathway genes and increased JA contents compared with the wild-type. Moreover, exogenous MeJA treatment induced cell death and ceramide accumulation in the mutant, and the loss of function of COI1 or JAR1 delayed the onset of cell death. We found that JAs modulate sphingolipid metabolism by triggering ceramide and hydroxyceramide accumulation, which is dependent on an intact JA pathway.

To investigate the connection between JA and the ceramide kinase ACD5, we measured the transcript levels of JA-related genes and the JA contents in *acd5* mutants. The *acd5* plants exhibited increased ceramide levels in late developmental stages, along with upregulated expression of the JA biosynthesis pathway gene *AOS* and accumulation of JAs (Figure 1; Bi et al., 2014), which suggested that endogenous ceramides promote JA synthesis. Moreover, the transcript level of *AOS* increased in response to treatment with exogenous ceramides (Figure 1), demonstrating that ceramides can promote the JA biosynthesis pathway.

JA induces defenses against plant-associated organisms, especially vertebrate herbivores. Mutation of *ACD5* had no effect on plant resistance to *S. exigua*, although the transcript

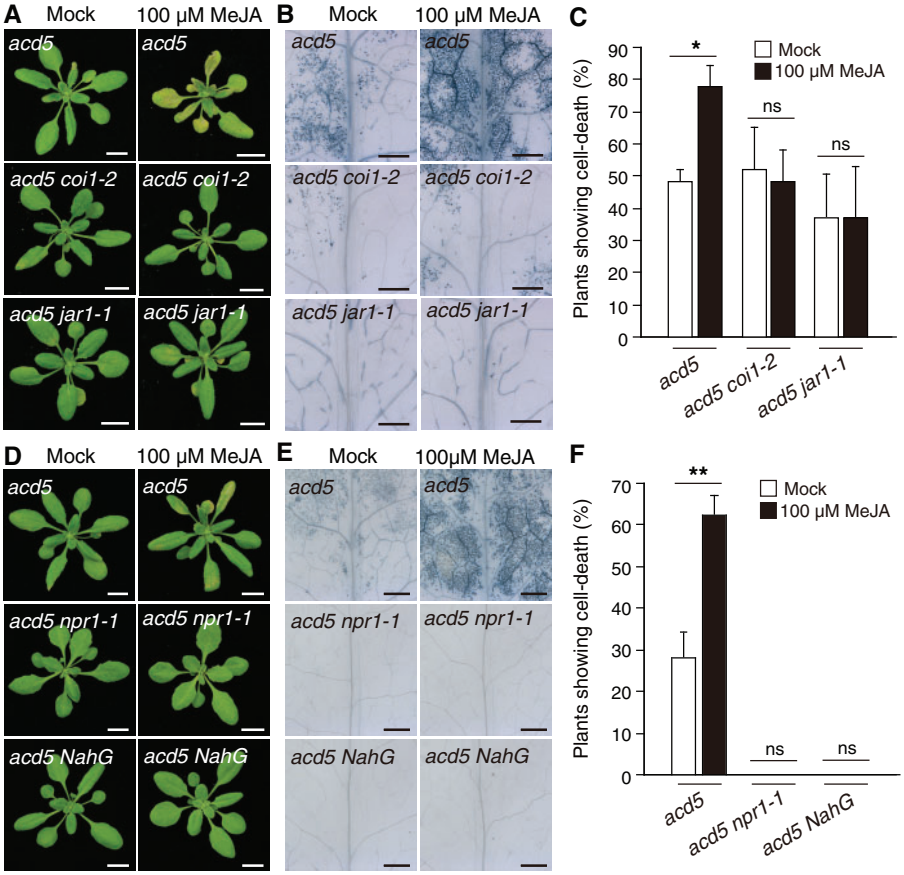

Figure 6 JA pathway and SA pathway are involved in JA-induced acceleration of cell death in *acd5*. Sixteen-day-old plants of the *acd5* and the indicated double mutants were sprayed with mock-treatment solution (0.1% ethanol) or 100-μM MeJA. Photographs (scale bars, 1 cm) were taken 8 d after spraying (A and D), and trypan blue staining (scale bars, 1 mm) was done at the same time (B and E). At least 27 plants were observed for each genotype when analyzing the ratio of plants showing cell death (C and F). Data represent means ± SE from three biological replicates. Significant differences between mock and 100-μM MeJA treated *acd5* were determined by Student's *t* tests (*$P < 0.05$; ** $P < 0.01$).

levels of JA pathway genes and the JA contents did increase. This phenomenon is very similar to previous reports showing that *acd5* uncouples defense-related responses during pathogen attack (Greenberg et al., 2000; Bi et al., 2014). One potential explanation is that, notwithstanding the activation of hormone pathways (include JA and SA), some defense responses were reduced in the *acd5* mutant. For instance, compared to the wild-type, *acd5* plants had smaller cell wall appositions and lower callose deposition and apoplastic reactive oxygen species levels when responding to *B. cinerea* (Bi et al., 2014). The JA pathway also acts in regulating root growth and anthocyanin accumulation (Chen et al., 2011; Qi et al., 2011). We found that for 10-d-old plants grown on medium with MeJA, the *acd5* mutant did not show more severe root growth inhibition and did not accumulate more anthocyanin than the wild-type, indicating that the JA pathway is not yet activated in *acd5* mutants at early stages of development.

The JA pathway is involved in cell death caused by various environmental stresses. For example, pretreating plants with MeJA before exposure to ozone (O_3) attenuates ozone-induced cell death, and JA mutants have elevated sensitivity to ozone (Rao et al., 2000). In contrast, cell death induced by the mycotoxin FB1 requires the JA signaling pathway (Asai et al., 2000; Zhang et al., 2015). Similarly, JA controls $^1O_2$-induced PCD, which is dependent on SA (Beaugelin et al., 2019). Our current results show that the JA pathway is involved in *acd5*-conferred cell death when the *acd5* plants were treated with exogenous MeJA (Figure 3), and MeJA induced cell death and sphingolipid accumulation in *acd5* mutants in a dose-dependent manner.

Sphingolipid-induced cell death is closely associated with hormone pathways, especially the SA pathway (Brodersen et al., 2002; Wang et al., 2008; Mortimer et al., 2013; Bi et al., 2014). Many reports suggest that the SA and JA signaling pathways play antagonistic roles in the regulation of plant resistance; however, the crosstalk between SA and JA signaling is complex during the induction of cell death. Mur et al (2006) reported that SA and JA synergize to induce cell death. Several other reports also revealed that the SA and JA pathways work together in processes such as $^1O_2$-induced cell death (Beaugelin et al., 2019) and cell death in mutants that lack neutral ceramidase (Zienkiewicz et al., 2019). In the case of *acd5* mutants, combining previous reports with the current data suggests that SA and JA may function synergistically in ceramide-induced cell death (Greenberg et al.,

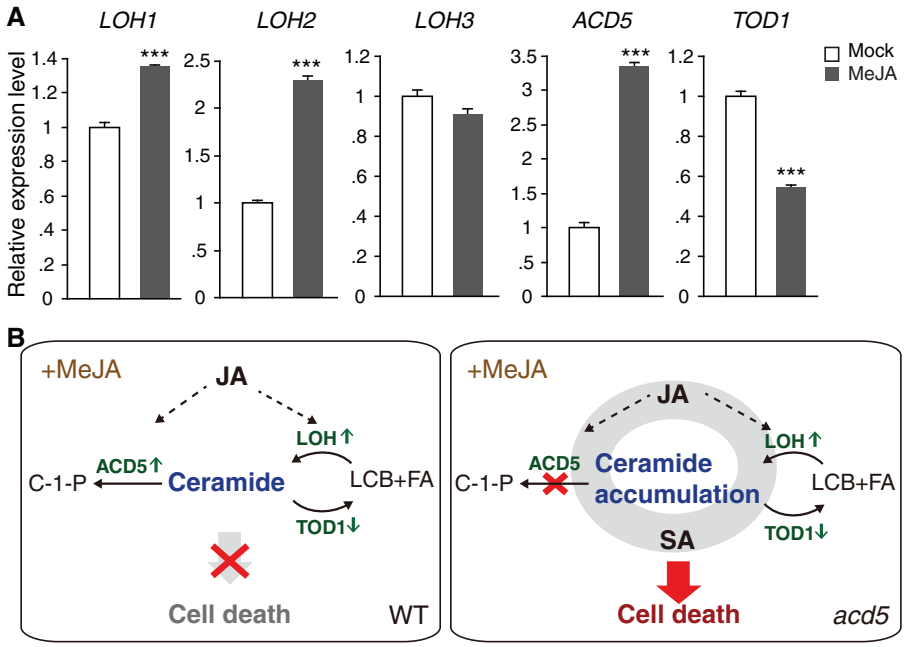

Figure 7 Expression of ceramide metabolism-related genes after MeJA treatment. A, Expression levels of ceramide metabolism-related genes in wild-type plants after MeJA treatment. Three-week-old wild-type plants were sprayed with mock-treatment solution (0.1% ethanol) or 100-μM MeJA. The samples were collected 6 h after MeJA treatment. The ceramide synthase genes *LOH1*, *LOH2*, and *LOH3*, the alkaline ceramidase gene *TOD1*, and *ACD5* were analyzed. *ACT2* transcript levels were used as the internal control. Gene expression values are relative to the average for mock-treated wild-type plants (set as 1). Significant differences between mock- and MeJA-treated plants were determined by Student's *t* tests (***$P < 0.001$). Data represent means ± SE using independent samples ($n = 3$). Experiments were repeated at least three times. B, Working model for JA regulation of sphingolipid metabolism and ceramide-associated-cell death in *acd5*. LOHs represent three ceramide synthase homologs; TOD1 degrades ceramides into LCBs and FAs. In wild-type plants, JA induced the expression of *LOH*s and suppressed the expression of *TOD1*, which might result in ceramide accumulation. However, the *ACD5* transcript level is upregulated, which may prevent excessive ceramide accumulation. In *acd5* mutants, the ceramide kinase is impaired, and high levels of ceramides accumulate, leading to SA-dependent cell death. We also found that JA biosynthesis and signaling are activated in *acd5* plants and ceramides can induce JA biosynthesis.

2000; Figure 4). Both SA and JAs accumulated in *acd5* plants, and SA- and JA-related genes were upregulated. However, the timing of the expression of SA and JA pathway genes in MeJA-treated plants occurs in a specific sequence. We found that during the early stages of MeJA treatment in the *acd5* mutant, JA-related genes were upregulated, but SA pathway genes were not, suggesting that the JA pathway plays an important role in the initiation of cell death in *acd5*. However, in later stages, the ceramide-induced cell death in *acd5* is predominantly dependent on the SA pathway (Greenberg et al., 2000; Bi et al., 2014; Yang et al., 2019).

Mutation of *MYC2* had no effect on cell death in *acd5* plants, but *coi1-2 and jar1-1* delayed the initial development of the *acd5* cell death phenotype: *acd5* plants showed cell death starting at 4 weeks, but *acd5 coi1-2 and acd5 jar1-1* plants showed cell death starting at 5 weeks. In contrast, *NahG and npr1-1* largely suppressed the cell death of *acd5*: cell death was absent in the *acd5 NahG* plants and was highly attenuated in the *acd5 npr1-1* plants (Greenberg et al., 2000). These observations indicated that inactivation of the JA pathway delayed cell death in *acd5* mutants, but inactivation of SA by *NahG* suppressed the cell death in *acd5* mutants (Greenberg et al., 2000; Yang et al., 2019). Based on these observations, we propose that *acd5*-conferred cell death is dependent on the SA pathway and partly dependent on the JA pathway. We speculated that JA acts upstream to accelerate the initiation of SA-dependent cell death in *acd5* plants.

Arabidopsis *NCER1* encodes a putative neutral ceramidase (Li et al., 2015; Zienkiewicz et al., 2019), and a T-DNA mutant of *NCER1* (SALK_054725) exhibits an increase in hydroxyceramides and an early leaf senescence phenotype that was partially suppressed by inactivation of JA-Ile biosynthesis, but completely suppressed by inactivation of the SA pathway (Zienkiewicz et al., 2019). Our findings are thus consistent with these earlier results. It is noteworthy that JAs induced the accumulation of ceramides (Figure 5), and age-dependent ceramide accumulation was observed in cell death mutants such as *acd5 and orm1* amiR-*ORM2* (Bi et al., 2014; Li et al., 2016). Furthermore, during leaf senescence, the JA level increased and genes associated with JA biosynthesis were upregulated (He et al., 2002). These results suggested that ceramide contents and JA levels increase during plant aging and JA possibly promotes the accumulation of ceramides in an age-dependent manner.

JAs mediate the biosynthesis of various metabolites, such as glucosinolates and anthocyanin (Qi et al., 2011; Schweizer et al., 2013; Wasternack and Strnad, 2019). We inferred that

JAs may induce cell death in *acd5* by mediating sphingolipid metabolism. To test this hypothesis, we treated wild-type plants with exogenous MeJA and found that this induced ceramide and hydroxyceramide accumulation. Interestingly, MeJA treatment did not effectively induce ceramide accumulation in *jar1-1 and coi1-2* mutants, but it caused *myc2-2* plants to accumulate the same levels of ceramides as the wild-type (Figure 5). Considering that MYC2, MYC3, and MYC4 are involved in regulating glucosinolate biosynthesis and insect resistance (Fernandez-Calvo et al., 2011; Schweizer et al., 2013), we speculated that MYC transcription factors function redundantly in regulating ceramide and hydroxyceramide contents. These results indicated that JAs regulate sphingolipid metabolism through a mechanism that requires intact JA signaling pathways. Moreover, we found that MeJA-induced cell death in *acd5* mutants was dependent on COI1 and JAR1 (Figure 6), which further demonstrated that JAs induce cell death in *acd5* by increasing the levels of ceramides. However, MeJA had no effect on the cell death phenotype of *acd5* in the absence of an intact SA pathway (Figure 6) again confirming that cell death in *acd5* is SA dependent.

JAs mediate plant secondary metabolism by regulating the expression of genes encoding enzymes in metabolic pathways (Wasternack and Strnad, 2019). Ceramides in Arabidopsis are regulated by several enzymes, such as ceramide synthases, ceramidases (TOD1), and ceramide kinases (ACD5); these enzymes play an important role in balancing ceramide metabolism (Liang et al., 2003; Ternes et al., 2011; Bi et al., 2014; Chen et al., 2015). We found that MeJA promoted the expression of *LOH1 and LOH2*, but repressed the transcription of *TOD1*, which might result in the accumulation of ceramides in Arabidopsis under MeJA treatment (Figures 5 and 7A). Moreover, MeJA induced the transcript level of *ACD5* (Figure 7A). We assumed that elevated expression of *ACD5* allows the plant to convert MeJA-induced ceramides into other derivatives and avoid cell death.

Analyzing the data from previous reports (Wang et al., 2019; Zander et al., 2020) indicated that the important transcription factor MYC2 may bind to the promoters of sphingolipid pathway genes such as *TOD1*, *LOH2*, and *ACD5*. Furthermore, the MYC2–MED25 transcriptional complex may regulate the transcription of sphingolipid pathway genes. These results supporting the idea that JAs regulate the expression of genes encoding enzymes in sphingolipid metabolism and thus alter ceramide homeostasis.

We summarize our current working model in Figure 7B. We found that JAs promote the accumulation of ceramides in wild-type plants, and this requires an intact JA pathway. In turn, ceramides enhance the expression of JA-related genes and JA levels. ACD5 is involved in balancing ceramide contents after JA treatment in wild-type plants. In the *acd5* mutant, ceramide kinase activity was disrupted, and ceramides induced by JA could not be converted to other derivatives, leading to excess accumulation of ceramides, which resulted in SA-dependent cell death. Thus, JA accelerates cell death in the *acd5* mutant. Taking these observations together, we speculated that the JA pathway mediates sphingolipid metabolism by affecting the expression of genes involved in ceramide metabolism. However, the mechanism whereby JA regulates the transcription of sphingolipid-related genes, and the functions of sphingolipids in plant–insect interaction, still need further investigation.

Materials and methods

Plants and growth conditions

The Arabidopsis (*A. thaliana*) reference accession Col-0 was used as the wild-type. Plants were grown on soil at 22°C under a 16-h light/8-h dark cycle with 6,000 lux light intensity. The mutants *jar1-1* (CS8072), *coi1-2*, and *myc2-2* (SALK_083483) have been described in previous studies (Staswick et al., 2002; Xiao et al., 2004; Boter et al., 2004). The *acd5 jar1-1*, *acd5 coi1-2*, and *acd5 myc2-2* double mutants were generated by crossing the T-DNA or point mutants into the *acd5* background (Greenberg et al., 2000; Bi et al., 2014). The *npr1-1*, *NahG*, *acd5 npr1-1*, and *acd5 NahG* mutants have been described previously (Greenberg et al., 2000).

RNA extraction and RT-qPCR

Total RNA was isolated using the E.Z.N.A. Plant RNA Kit (R6827-01, Omega Bio-tek) according to the manufacturer's instructions. Total RNA (1 μg) was reverse-transcribed in a 20-μL reaction mixture using the PrimeScript RT reagent Kit (Takara, RR047A). RT-qPCR was performed with the SYBR Premix ExTaqkit (Takara, RR820L) and analyzed using a LightCycler480 Real-Time PCR System (Roche). We used the $2^{-\Delta\Delta Ct}$ method (Livak and Schmittgen, 2001) to determine the expression level of target genes relative to *ACT2*. The primers used are listed in Supplemental Table S1.

Hormone measurements

Phytohormones were extracted following the method in Pan et al. (2010). Briefly, fresh leaf tissue was ground using liquid nitrogen. The powdered samples (~200 mg) were sealed in 2-mL tubes containing 0.9-mL extraction buffer (2:1:0.002 [v/v/v] isopropanol: water: concentrated HCl) with internal standards ($^2H_5$-JA and $^2H_4$-SA, Olchemim). The samples were gently mixed for 30 min at 4°C, and then 0.9-mL dichloromethane was added to each sample and the samples were shaken for 30 min at 4°C. The mixtures were centrifuged at 13,000*g* for 5 min. One milliliter of solvent from the lower phase was dried using a nitrogen evaporator. The samples were dissolved in a 200-μL solution containing 120-μL methanol and 80-μL distilled water. Ten microliters of each sample were injected into a C18 column and analyzed using the AB SCIEX Triple TOF 5600+ system as described previously (Yuan et al., 2017).

Exogenous ceramide treatment

C2- and C16-ceramide were dissolved in ethanol and prepared as 5-mM stock solutions. Seedlings were grown

vertically on plates containing half-strength Murashige and Skoog (1/2 MS) medium for 7 d and then transferred to 1/2 MS liquid medium in the presence of 50-μM C2- or C16-ceramide in 1% ethanol. Control plants were transferred to 1/2 MS liquid medium containing 1% ethanol.

Combination treatment of Arabidopsis protoplasts

MeJA (Sigma-Aldrich) was dissolved in ethanol and prepared as a 10-mM stock solution. C2-ceramides were dissolved in ethanol and prepared as 5-mM stock solutions. The fluorescein diacetate (FDA) was dissolved in acetone and prepared as a 5 $mg{\cdot}mL^{-1}$ stock solution. The protoplasts were isolated from 3-week-old wild-type plants using the method described in a previous study (Yoo et al., 2007). The protoplasts were treated with mock-treatment solution (1% ethanol), 100-μM MeJA, or 50-μM C2-ceramide under light. After 24 h of treatment, the protoplasts were incubated in 50 $\mu g{\cdot}mL^{-1}$ FDA for 3 min and observed with confocal microscopy (LSM-880; Carl Zeiss). The excitation/emission wavelengths were: 488 nm/493–567 nm for GFP; 633 nm/649–721 nm for chlorophyll. Laser intensity was adapted in the 2%. Gains were optimized and kept consistent throughout the experiment.

Insect feeding assay and fungal infection

Spodoptera exigua larvae (2nd instar) were purchased from Dr Kai Yang (Sun Yat-sen University). Two larvae were reared on each plant per genotype. At least twenty 4-week-old plants per genotype were used for the assay. After 8 d of feeding, *S. exigua* larvae were weighed and then killed in 75% (v/v) methanol for photographic documentation.

Botrytis cinerea was cultured on potato dextrose agar plates at 25°C for 15 d. Spores were washed and collected in Vogel buffer containing 20-mM K_2HPO_4, 20-mM NH_4NO_3, 1-mM $MgSO_4$, 10-mM $CaCl_2$, 50-mM sucrose, and 10-mM sodium citrate. For inoculation, the fungal spore density was adjusted to 10^7 spores mL^{-1} and sprayed on 21-d-old plants. The inoculated plants were protected by a transparent cover to maintain high humidity for 2 d and incubated for 24 h under darkness. Then, the plants were shifted to a 16-h light/8-h dark photoperiod regime.

Exogenous hormone treatments and root growth inhibition assay

MeJA (Sigma-Aldrich) was dissolved in ethanol and prepared as a 50-, 100-, or 200-mM stock solution. Plants grown in soil were sprayed with mock-treatment solution (0.1% ethanol) or 50-, 100-, or 200-μM MeJA and then kept under a transparent cover overnight.

For the root growth inhibition assay, seedlings were grown vertically on plates containing 1/2 MS medium in the presence or absence of 100-μM MeJA for 10 d and then photographed. Primary root length was measured using ImageJ software (National Institutes of Health, version 1.47).

Anthocyanin analysis

The wild-type and *acd5* plants were grown on 1/2 MS medium in the presence or absence of 100-μM MeJA for 10 d. The anthocyanin analysis method has been described previously (Zheng et al., 2018). Briefly, the samples (∼50 mg) were submerged in methanol containing 1% (v/v) HCl solution at 4°C overnight. After extraction, 400-μL water and 400-μL chloroform were added and mixed. The mixtures were centrifuged at 12,000 rpm for 2 min and the supernatant collected. The absorbance (A) of the supernatant was measured at 530 and 657 nm, and the anthocyanin content was determined using the formula $(A_{530} - 1/4A_{657})/FW$.

Trypan blue staining

Trypan blue staining assay was described in Yang et al. (2019). Briefly, plant leaves were submerged in the trypan blue solution containing 2.5-$mg{\cdot}mL^{-1}$ trypan blue (Sigma-Aldrich), 25% (v/v) lactic acid, 25% (v/v) water-saturated phenol, 25% (v/v) glycerol, and 25% (v/v) distilled water. The samples were heated in boiling water for 1 min and then decolorized in a chloral hydrate solution (2.5-g chloral hydrate dissolved in 1-mL distilled water) for at least 10 h. The leaves were stored in 50% (v/v) glycerol and observed with a stereomicroscope.

Sphingolipid analysis

Samples for sphingolipid analysis were prepared as described in Li et al. (2016). Briefly, 30 mg of lyophilized samples were extracted using a mixture of isopropanol/hexane/water (55:20:25; v/v/v) containing internal standards (d17:1-sphingosine, d18:1/12:0-ceramide, d18:1/12:0-glucosylceramide, G_{M1} ganglioside) and incubated at 60°C for 15 min. After centrifugation, the supernatant was dried under nitrogen and de-esterified in 33% methylamine in ethanol/water (7:3, v/v) for 1 h at 50°C. The samples were dried, dissolved in 250-μL methanol, and analyzed using the hybrid quadrupole time-of-flight mass spectrometer (AB SCIEX Triple TOF 5600+) with a Phenomenex Luna C8 column (150 mm × 2.0 mm, 3 μm). The samples for GIPC detection were dissolved in a 250-μL mixture of methanol/tetrahydrofuran/water (1:2:2; v/v/v) and analyzed using the Triple Quadrupole mass spectrometer (Agilent 6410 Triple Quadrupole LC/MS system).

Electrolyte leakage

Electrolyte leakage was determined as described in Yuan et al. (2017). The wild-type and *acd5* plants treated with different concentrations of MeJA for 10 d were submerged in deionized water and gently agitated for 1 h. The conductivity of the solution was measured, and it was then heated in boiling water for 10 min. After it cooled to room temperature, total electrolyte strength was recorded. The relative electrolyte leakage was calculated by comparing the leaked ionic strength with the corresponding total ionic strength.

Protoplast transfection assay

For generating effector constructs, the coding sequence of *MYC2* was cloned into pX-DG-GFP. For generating the $ACD5_{Pro}$-*LUC* reporter construct, the upstream ~1,700-bp promoter sequence of *ACD5* was cloned into the pGreenII 0800-LUC vector. The protoplast preparation and subsequent transfection have been described previously (Yoo et al., 2007), and 10 mg of reporter and effector plasmids were used. The firefly LUC and Renilla luciferase activities were measured with the Dual-Luciferase Reporter Assay System (Promega) using Tecan-Spark.

Statistical analyses

Data represent means ± SE. Significant differences were determined by analysis of variance (ANOVA) post hoc tests in conjunction with Fisher's protected least significant difference test ($P < 0.05$, $P < 0.01$) using different letters or determined by Student's *t* test ($^{*}P < 0.05$, $^{**}P < 0.01$, $^{***}P < 0.001$). The number of biological replicates is given in the figure legends.

Accession numbers

Sequence data discussed in this article can be found in the Arabidopsis Genome Initiative database under the following accession numbers: *AOS* (AT5G42650), *AOC1* (AT3G25760), *AOC2* (AT3G25770), *OPR3* (AT2G06050), *JAR1* (AT2G46370), *JAZ1* (AT1G19180), *MYC2* (AT1G32640), *PDF1.2* (AT5G44420), *ACD5* (AT5G51290), *COI1* (AT2G39940), *JAZ10* (AT5G13220), *TAT1* (AT5G53970), *JAZ7* (AT2G34600), *JAZ8* (AT1G30135), *SID2* (AT1G74710), *NPR1* (AT1G64280), *EDS1* (AT3G48090), *PAD4* (AT3G52430), *PR1* (AT2G14610), *LOH1* (AT3G25540), *LOH2* (AT3G19260), *LOH3* (AT1G13580), *TOD1* (AT5G46220), *PR2* (AT3G57260), *PR5* (AT1G75040), *SAG12* (AT5G45890), *SAG13* (AT2G29350), *SAG113* (AT5G59220), *APX2* (AT3G09640), *BAP1* (AT3G61190), *MED25* (AT1G25540), and *ACTIN2* (AT3G18780).

Supplemental data

The following materials are available in the online version of this article.

Supplemental Figure S1. Levels of SA and SAG in 16- and 32-d-old wild-type and *acd5* plants.

Supplemental Figure S2. The response to *B. cinerea* in the wild-type and *acd5* plants.

Supplemental Figure S3. Effect of MeJA treatments on the cell death phenotype of *acd5*.

Supplemental Figure S4. The expression of defense, senescence, and reactive oxygen species-related genes in *acd5* after MeJA treatment.

Supplemental Figure S5. The hormone levels of JA and SA in the wild-type and *acd5* plants after MeJA treatment.

Supplemental Figure S6. The effects of ceramide and MeJA on Arabidopsis protoplasts.

Supplemental Figure S7. SA- and JA-related gene expression in *acd5* after MeJA treatment.

Supplemental Figure S8. Identifications and phenotypes of *acd5 myc2-2*, *acd5 coi1-2*, and *acd5 jar1-1* mutants.

Supplemental Figure S9. Ceramide and hydroxyceramide contents in JA pathway mutants after MeJA treatment.

Supplemental Figure S10. Effect of 100-μM MeJA on the phenotypes of the wild-type, JA mutants, and SA mutants.

Supplemental Figure S11. The expression of genes related to ceramide metabolism in *acd5* after MeJA treatment.

Supplemental Figure S12. The MYC2 transcription factor is involved in regulating the expression of sphingolipid pathway gene *ACD5*.

Supplemental Table S1. Primers used in this study.

Funding

This work was supported by grants from the National Natural Science Foundation of China (31771357, 32070196), the Natural Science Foundation of Guangdong Province (2019B1515120088; 2018A030313360), the China Postdoctoral Science Foundation (2016M592575), and Sun Yat-sen University (Project 33000-31143406).

Conflict of interest statement. The authors declare no conflict interest.

References

Ali U, Li H, Wang X, Guo L (2018) Emerging roles of sphingolipid signaling in plant response to biotic and abiotic stresses. Mol Plant **11:** 1328–1343

An C, Li L, Zhai Q, You Y, Deng L, Wu F, Chen R, Jiang H, Wang H, Chen Q, Li C (2017) Mediator subunit MED25 links the jasmonate receptor to transcriptionally active chromatin. Proc Natl Acad Sci USA **114:** E8930–E8939

Asai T, Stone JM, Heard JE, Kovtun Y, Yorgey P, Sheen J, Ausubel FM (2000) Fumonisin B1–induced cell death in Arabidopsis protoplasts requires jasmonate-, ethylene-, and salicylate-dependent signaling pathways. Plant Cell **12:** 1823–1836

Beaugelin I, Chevalier A, D'Alessandro S, Ksas B, Novak O, Strnad M, Forzani C, Hirt H, Havaux M, Monnet F (2019) OXI1 and DAD regulate light-induced cell death antagonistically through jasmonate and salicylate levels. Plant Physiol **180:** 1691–1708

Begum MA, Shi XX, Tan Y, Zhou WW, Hannun Y, Obeid L, Mao C, Zhu ZR (2016) Molecular characterization of rice *OsLCB2a1* gene and functional analysis of its role in insect resistance. Front Plant Sci **7:** 1789

Berkey R, Bendigeri D, Xiao S (2012) Sphingolipids and plant defense/disease: the "death" connection and beyond. Front Plant Sci **3:** 68

Bi FC, Liu Z, Wu JX, Liang H, Xi XL, Fang C, Sun TJ, Yin J, Dai GY, Rong C, et al. (2014) Loss of ceramide kinase in Arabidopsis impairs defenses and promotes ceramide accumulation and mitochondrial H_2O_2 bursts. Plant Cell **26:** 3449–3467

Boter M, Ruíz-Rivero O, Abdeen A, Prat S (2004) Conserved MYC transcription factors play a key role in jasmonate signaling both in tomato and Arabidopsis. Genes Dev **18:** 1577–1591

Brodersen P, Petersen M, Pike HM, Olszak B, Skov S, Odum N, Jørgensen LB, Brown RE, Mundy J (2002) Knockout of Arabidopsis *ACCELERATED-CELL-DEATH11* encoding a sphingosine transfer protein causes activation of programmed cell death and defense. Genes Dev **16:** 490–502

Chen R, Jiang H, Li L, Zhai Q, Qi L, Zhou W, Liu X, Li H, Zheng W, Sun J, Li C (2012) The Arabidopsis mediator subunit MED25 differentially regulates jasmonate and abscisic acid signaling through interacting with the MYC2 and ABI5 transcription factors. Plant Cell **24:** 2898–2916

Chen Q, Sun J, Zhai Q, Zhou W, Qi L, Xu L, Wang B, Chen R, Jiang H, Qi J, et al. (2011) The basic helix-loop-helix transcription factor MYC2 directly represses *PLETHORA* expression during

jasmonate-mediated modulation of the root stem cell niche in Arabidopsis. Plant Cell **23:** 3335–3352

Chen LY, Shi DQ, Zhang WJ, Tang ZS, Liu J, Yang WC (2015) The Arabidopsis alkaline ceramidase TOD1 is a key turgor pressure regulator in plant cells. Nat Commun **6:** 6030

Du M, Zhao J, Tzeng DTW, Liu Y, Deng L, Yang T, Zhai Q, Wu F, Huang Z, Zhou M, et al. (2017) MYC2 orchestrates a hierarchical transcriptional cascade that regulates jasmonate-mediated plant immunity in tomato. Plant Cell **29:** 1883–1906

Fernandez-Calvo P, Chini A, Fernandez-Barbero G, Chico JM, Gimenez-Ibanez S, Geerinck J, Eeckhout D, Schweizer F, Godoy M, Franco-Zorrilla JM, et al. (2011) The *Arabidopsis* bHLH transcription factors MYC3 and MYC4 are targets of JAZ repressors and act additively with MYC2 in the activation of jasmonate responses. Plant Cell **23:** 701–715

Fonseca S, Chini A, Hamberg M, Adie B, Porzel A, Kramell R, Miersch O, Wasternack C, Solano R (2009) (+)-7-*iso*-Jasmonoyl-$_L$-isoleucine is the endogenous bioactive jasmonate. Nat Chem Biol **5:** 344–350

Greenberg JT, Silverman FP, Liang H (2000) Uncoupling salicylic acid-dependent cell death and defense-related responses from disease resistance in the Arabidopsis mutant *acd5*. Genetics **156:** 341–350

He Y, Fukushige H, Hildebrand DF, Gan S (2002) Evidence supporting a role of jasmonic acid in Arabidopsis leaf senescence. Plant Physiol **128:** 876–884

Howe GA, Major IT, Koo AJ (2018) Modularity in jasmonate signaling for multistress resilience. Annu Rev Plant Biol **69:** 387–415

Li J, Bi FC, Yin J, Wu JX, Rong C, Wu JL, Yao N (2015) An Arabidopsis neutral ceramidase mutant *ncer1* accumulates hydroxyceramides and is sensitive to oxidative stress. Front Plant Sci **6:** 460

Li J, Yin J, Rong C, Li KE, Wu JX, Huang LQ, Zeng HY, Sahu SK, Yao N (2016) Orosomucoid proteins interact with the small subunit of serine palmitoyltransferase and contribute to sphingolipid homeostasis and stress responses in Arabidopsis. Plant Cell **28:** 3038–3051

Liang H, Yao N, Song JT, Luo S, Lu H, Greenberg JT (2003) Ceramides modulate programmed cell death in plants. Genes Dev **17:** 2636–2641

Liu Y, Du M, Deng L, Shen J, Fang M, Chen Q, Lu Y, Wang Q, Li C, Zhai Q (2019) MYC2 regulates the termination of jasmonate signaling via an autoregulatory negative feedback loop. Plant Cell **31:** 106–127

Livak KJ, Schmittgen TD (2001) Analysis of relative gene expression data using real-time quantitative PCR and the 2(-Delta Delta C(T)) method. Methods **25:** 402–408

Luttgeharm KD, Kimberlin AN, Cahoon EB (2016) Plant sphingolipid metabolism and function. Subcell Biochem **86:** 249–286

Magnin-Robert M, Le Bourse D, Markham J, Dorey S, Clement C, Baillieul F, Dhondt-Cordelier S (2015) Modifications of sphingolipid content affect tolerance to Hemibiotrophic and Necrotrophic pathogens by modulating plant defense responses in Arabidopsis. Plant Physiol **169:** 2255–2274

Mortimer JC, Yu X, Albrecht S, Sicilia F, Huichalaf M, Ampuero D, Michaelson LV, Murphy AM, Matsunaga T, Kurz S, et al. (2013) Abnormal glycosphingolipid mannosylation triggers salicylic acid-mediated responses in Arabidopsis. Plant Cell **25:** 1881–1894

Mur LAJ, Kenton P, Atzorn R, Miersch O, Wasternack C (2006) The outcomes of concentration-specific interactions between salicylate and jasmonate signaling include synergy, antagonism, and oxidative stress leading to cell death. Plant Physiol **140:** 249–262

Pan X, Welti R, Wang X (2010) Quantitative analysis of major plant hormones in crude plant extracts by high-performance liquid chromatography-mass spectrometry. Nat Protoc **5:** 986–992

Qi T, Song S, Ren Q, Wu D, Huang H, Chen Y, Fan M, Peng W, Ren C, Xie D (2011) The Jasmonate-ZIM-domain proteins interact with the WD-Repeat/bHLH/MYB complexes to regulate Jasmonate-mediated anthocyanin accumulation and trichome initiation in *Arabidopsis thaliana*. Plant Cell **23:** 1795–1814

Rao MV, Lee H, Creelman RA, Mullet JE, Davis KR (2000) Jasmonic acid signaling modulates ozone-induced hypersensitive cell death. Plant Cell **12:** 1633–1646

Schweizer F, Fernandez-Calvo P, Zander M, Diez-Diaz M, Fonseca S, Glauser G, Lewsey MG, Ecker JR, Solano R, Reymond P (2013) Arabidopsis basic helix-loop-helix transcription factors MYC2, MYC3, and MYC4 regulate glucosinolate biosynthesis, insect performance, and feeding behavior. Plant Cell **25:** 3117–3132

Simanshu DK, Zhai X, Munch D, Hofius D, Markham JE, Bielawski J, Bielawska A, Malinina L, Molotkovsky JG, Mundy JW, et al. (2014) Arabidopsis accelerated cell death 11, ACD11, is a ceramide-1-phosphate transfer protein and intermediary regulator of phytoceramide levels. Cell Rep **6:** 388–399

Staswick PE, Tiryaki I, Rowe ML (2002) Jasmonate response locus *JAR1* and several related Arabidopsis genes encode enzymes of the firefly luciferase superfamily that show activity on jasmonic, salicylic, and indole-3-acetic acids in an assay for adenylation. Plant Cell **14:** 1405–1415

Ternes P, Feussner K, Werner S, Lerche J, Iven T, Heilmann I, Riezman H, Feussner I (2011) Disruption of the ceramide synthase LOH1 causes spontaneous cell death in *Arabidopsis thaliana*. New Phytol **192:** 841–854

Thines B, Katsir L, Melotto M, Niu Y, Mandaokar A, Liu G, Nomura K, He SY, Howe GA, Browse J (2007) JAZ repressor proteins are targets of the SCF(COI1) complex during jasmonate signalling. Nature **448:** 661–665

Townley HE, McDonald K, Jenkins GI, Knight MR, Leaver CJ (2005) Ceramides induce programmed cell death in Arabidopsis cells in a calcium-dependent manner. Biol Chem **386:**161–166

Wang H, Li S, Li Y, Xu Y, Wang Y, Zhang R, Sun W, Chen Q, Wang XJ, Li C, Zhao J (2019) MED25 connects enhancer-promoter looping and MYC2-dependent activation of jasmonate signalling. Nat Plants **5:** 616–625

Wang W, Yang X, Tangchaiburana S, Ndeh R, Markham JE, Tsegaye Y, Dunn TM, Wang GL, Bellizzi M, Parsons JF, et al. (2008) An inositolphosphorylceramide synthase is involved in regulation of plant programmed cell death associated with defense in Arabidopsis. Plant Cell **20:** 3163–3179

Wasternack C, Strnad M (2019) Jasmonates are signals in the biosynthesis of secondary metabolites - pathways, transcription factors and applied aspects - a brief review. N Biotechnol **48:** 1–11

Xiao S, Dai L, Liu F, Wang Z, Peng W, Xie D (2004) COS1: an Arabidopsis *coronatine insensitive1* suppressor essential for regulation of jasmonate-mediated plant defense and senescence. Plant Cell **16:** 1132–1142

Xie DX, Feys BF, James S, Nieto-Rostro M, Turner JG (1998) COI1: an Arabidopsis gene required for jasmonate-regulated defense and fertility. Science **280:** 1091–1094

Yan J, Zhang C, Gu M, Bai Z, Zhang W, Qi T, Cheng Z, Peng W, Luo H, Nan F, et al. (2009) The Arabidopsis CORONATINE INSENSITIVE1 protein is a jasmonate receptor. Plant Cell **21:** 2220–2236

Yang YB, Yin J, Huang LQ, Li J, Chen DK, Yao N (2019) Salt enhances disease resistance and suppresses cell death in ceramide kinase mutants. Plant Physiol **181:** 319–331

Yuan LB, Dai YS, Xie LJ, Yu LJ, Zhou Y, Lai YX, Yang YC, Xu L, Chen QF, Xiao S (2017) Jasmonate regulates plant responses to postsubmergence reoxygenation through transcriptional activation of antioxidant synthesis. Plant Physiol **173:** 1864–1880

Yoo SD, Cho YH, Sheen J (2007) Arabidopsis mesophyll protoplasts: a versatile cell system for transient gene expression analysis. Nat Protoc **2:** 1565–1572

Zander M, Lewsey MG, Clark NM, Yin L, Bartlett A, Guzmán JPS, Hann E, Langford AE, Jow B, Wise A, et al. (2020) Integrated multi-omics framework of the plant response to jasmonic acid. Nat Plants **6:** 290–302

Zhang X, Wu Q, Cui S, Ren J, Qian W, Yang Y, He S, Chu J, Sun X, Yan C, et al. (2015) Hijacking of the jasmonate pathway by the mycotoxin fumonisin B1 (FB1) to initiate programmed cell death in Arabidopsis is modulated by RGLG3 and RGLG4. J Exp Bot **66:** 2709–2721

Zheng P, Wu JX, Sahu SK, Zeng HY, Huang LQ, Liu Z, Xiao S, Yao N (2018) Loss of alkaline ceramidase inhibits autophagy in Arabidopsis and plays an important role during environmental stress response. Plant Cell Environ **41:** 837–849

Zienkiewicz A, Gömann J, König S, Herrfurth C, Liu YT, Meldau D, Feussner I (2019) Disruption of Arabidopsis neutral ceramidases 1 and 2 results in specific sphingolipid imbalances triggering different phytohormone-dependent plant cell death programmes. New Phytol **226:** 170–188